

# **Control Synthesis of Porous Single-Atomic Fe-N-C Catalyst with Fe Nanocluster as Synergistic Catalytic Sites for Efficient Oxygen Reduction**

Lili Fan,<sup>‡\*a</sup> Ling Zhang,<sup>‡a</sup> Xuting Li,<sup>a</sup> Hao Mei,<sup>a</sup> Mengfei Li,<sup>a</sup> Zhanning Liu,<sup>a</sup> Zixi Kang,<sup>a</sup> Yongxiao Tuo,<sup>\*b</sup> Rongming Wang,<sup>a</sup> and Daofeng Sun<sup>a</sup>

<sup>a</sup>School of Materials Science and Engineering, College of Science, China University of Petroleum (East China), Qingdao 266580, China

<sup>b</sup>College of New Energy, China University of Petroleum (East China), Qingdao, 266580, China

<sup>‡</sup>These authors contributed equally.

\*Corresponding authors (lilifan@upc.edu.cn; yxtuo@upc.edu.cn)

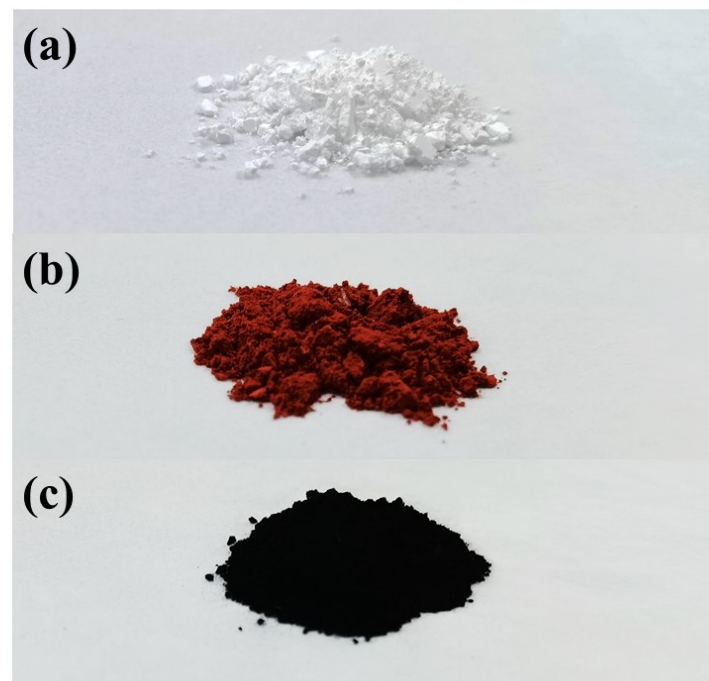


**Fig. S1** Digital photos of (a)  $\text{SiO}_2$  template, (b)  $\text{Fe-phen}@\text{SiO}_2\text{-7}$  and (c)  $\text{Fe(0)}/\text{FeN}_x\text{-NC-7}$ .

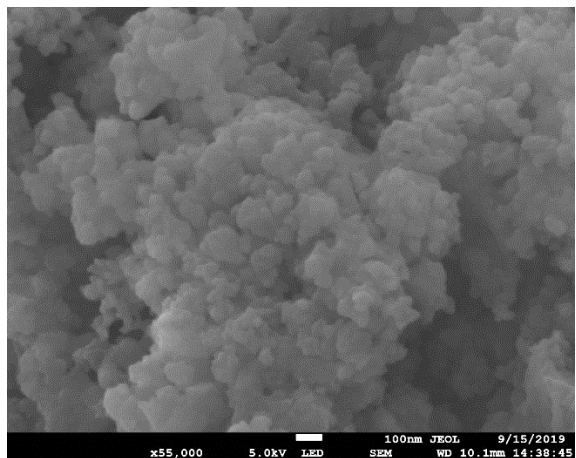


**Fig. S2** SEM image of SiO<sub>2</sub> template.

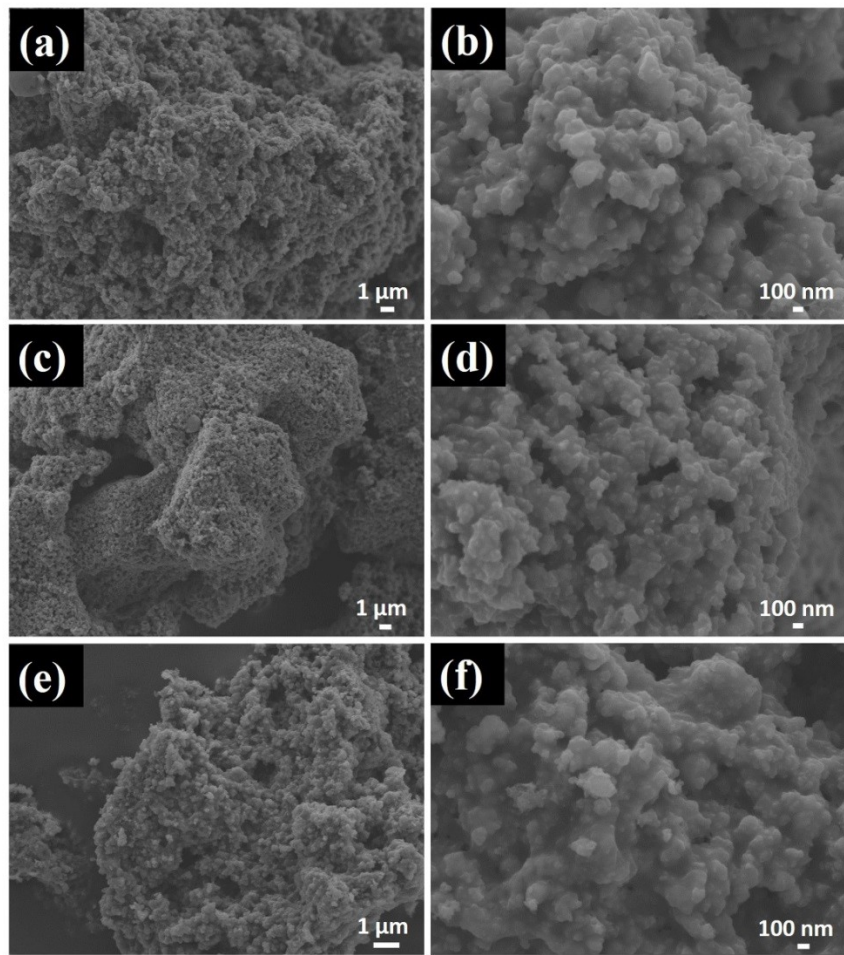


**Fig. S3** SEM images of (a, b) Fe-Phen@SiO<sub>2</sub>-6, (c, d) Fe-Phen@SiO<sub>2</sub>-7 and (e, f) Fe-Phen@SiO<sub>2</sub>-8.

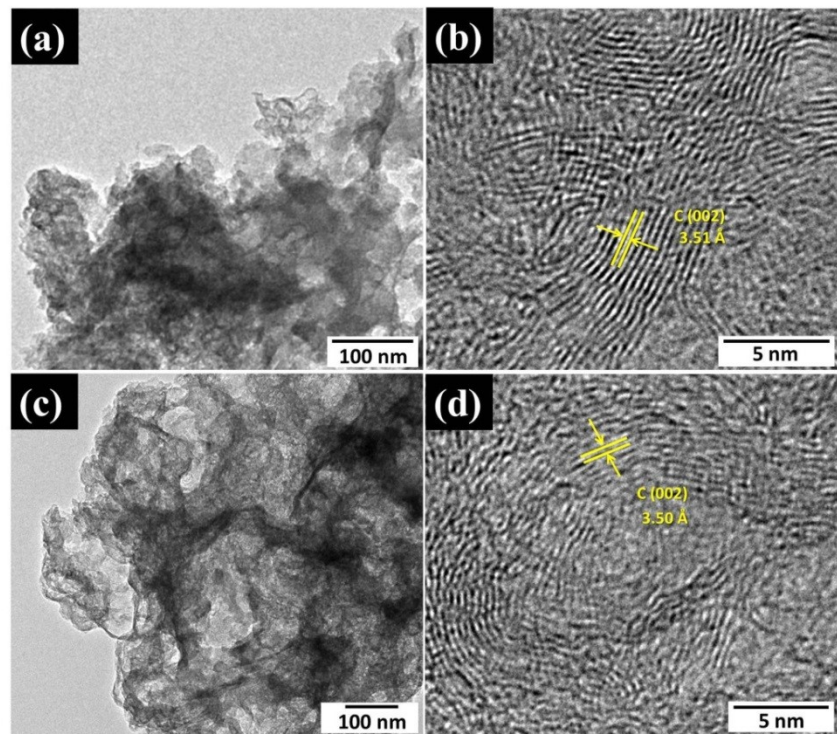


**Fig. S4** TEM images of (a, b) Fe(0)/FeN<sub>x</sub>-NC-6 and (c, d) Fe(0)/FeN<sub>x</sub>-NC-8.

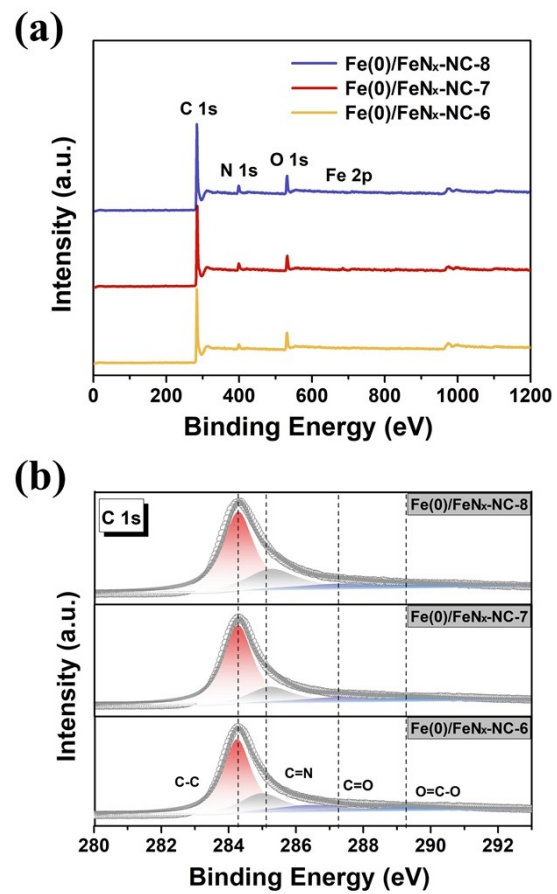


**Fig. S5** (a) XPS survey spectra and (b) C 1s high-resolution XPS spectra of Fe(0)/FeNx-NC-6, Fe(0)/FeNx-NC-7 and Fe(0)/FeNx-NC-8.

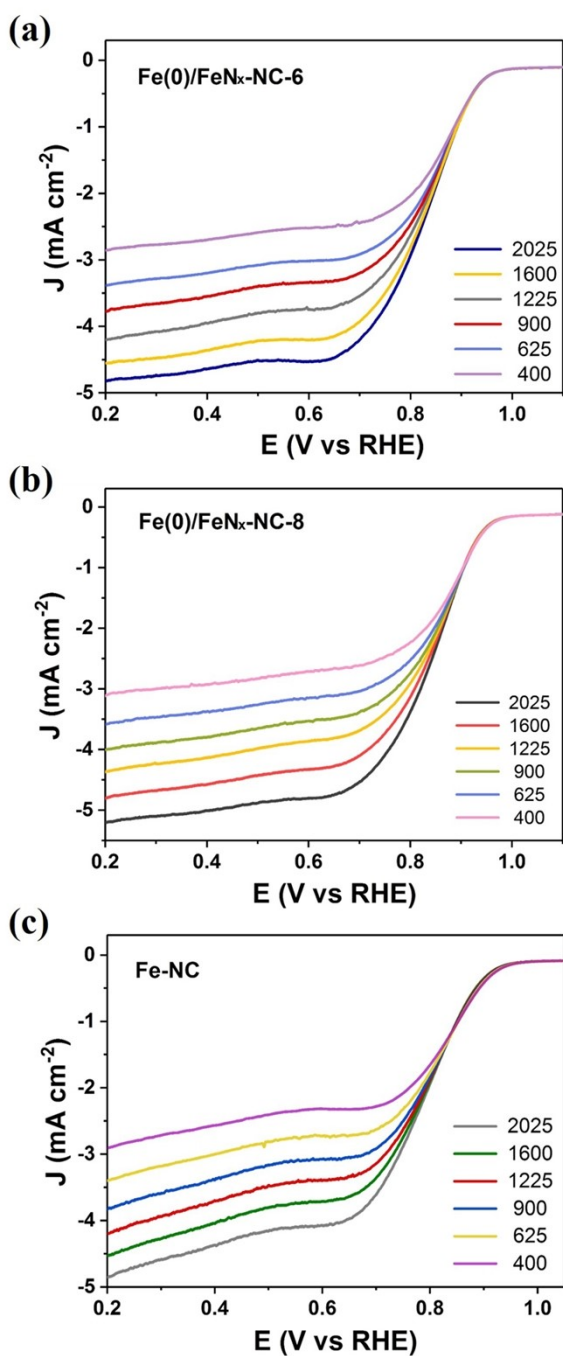


**Fig. S6** LSV curves of (a)  $\text{Fe}(0)/\text{FeN}_x\text{-NC-6}$ , (b)  $\text{Fe}(0)/\text{FeN}_x\text{-NC-8}$  and (c)  $\text{Fe-NC}$  at different rotating rates in  $\text{O}_2$ -saturated 0.1 M KOH solution.

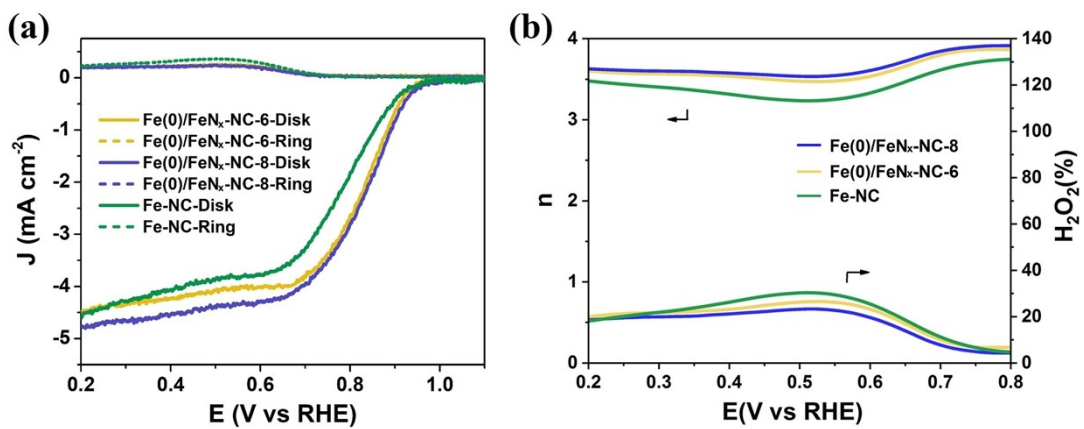


**Fig. S7** (a) RRDE tests at 1600 rpm in O<sub>2</sub>-saturated 0.1 M KOH solution and corresponding (b) electron transfer number (n) and H<sub>2</sub>O<sub>2</sub> yields of Fe(0)/FeN<sub>x</sub>-NC-6, Fe(0)/FeN<sub>x</sub>-NC-8, and Fe-NC.

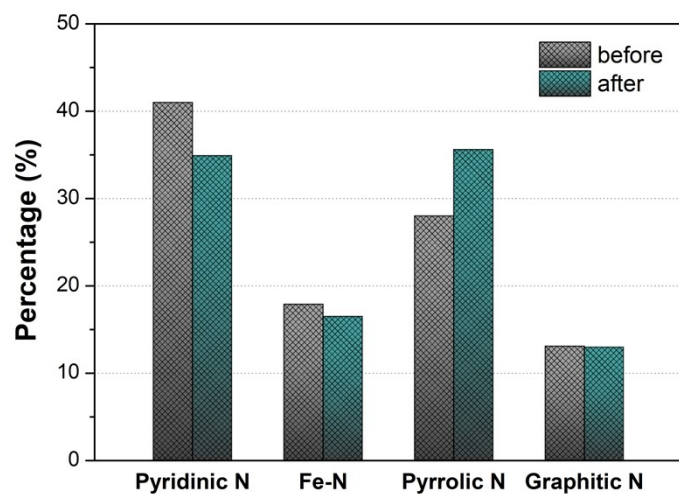


**Fig. S8** Percentage of different N species in Fe(0)/FeN<sub>x</sub>-NC-7 before and after 3000 CV cycles.

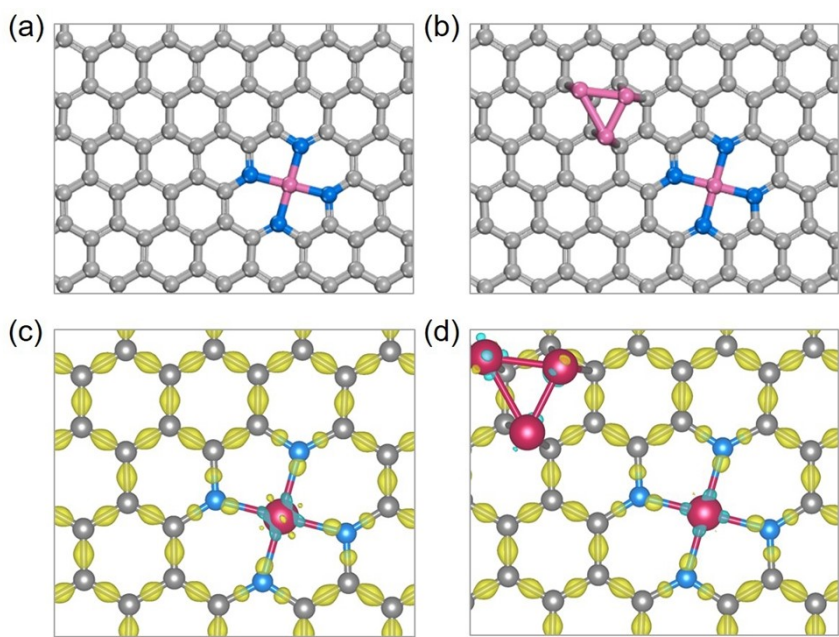


**Fig. S9** Optimized geometry of (a)  $\text{FeN}_4$  and (b)  $\text{Fe}_3\text{-FeN}_4$  systems. Three-dimensional charge density distributions of (c)  $\text{FeN}_4$  and (d)  $\text{Fe}_3\text{-FeN}_4$  systems. Electrons accumulation and depletion is in yellow and blue, respectively. The isosurfaces are all set to  $0.1 \text{ eV}\cdot\text{\AA}^{-3}$ .

**Table S1** Comparison of the ORR activity in alkaline solution of Fe(0)/FeN<sub>x</sub>-NC-7 with recently reported electrocatalysts.

Catalyst	Half-wave Potential (V)	Diffusion-Limited Current Density (mA cm <sup>-2</sup> )	Onset Potential (V)	Electrolyte	Ref.
Fe(0)/FeN <sub>x</sub> -NC-7	0.86	5.11	0.95	0.1 M KOH	This work
Fe/Meso-NC-1000	0.885	6.4	0.97	0.1 M KOH	Ref <sup>1</sup>
Fe-N/P-C-700	0.867	5.6	0.94	0.1 M KOH	Ref <sup>2</sup>
P-FeNCNW	0.858	5.9	0.93	0.1 M KOH	Ref <sup>3</sup>
FeSA-NSC-900	0.86	5.75	0.94	0.1 M KOH	Ref <sup>4</sup>
Fe-N-C	0.846	5.7	0.965	0.1 M KOH	Ref <sup>5</sup>
Fe/N/C-1000-0.05	0.86	5.3	0.98	0.1 M KOH	Ref <sup>6</sup>
FeCNR-750	0.83	5.10	0.96	0.1 M KOH	Ref <sup>7</sup>
Fe <sub>3</sub> /Co <sub>1</sub> -N-C	0.82	5.48	0.87	0.1 M KOH	Ref <sup>8</sup>
Fe/N/C-48-950-1	0.86	4.8	0.99	0.1 M KOH	Ref <sup>9</sup>
Fe/NC-NaCl	0.832	5.2	0.96	0.1 M KOH	Ref <sup>10</sup>
Fe-N-C-700	0.83	5.5	0.91	0.1 M KOH	Ref <sup>11</sup>
Fe-N-CPNS	0.84	5.8	-	0.1 M KOH	Ref <sup>12</sup>
Fe@N-C NT/NSs	0.79	7.2	0.96	0.1 M KOH	Ref <sup>13</sup>
Fe-N-3DPC-1000	0.85	5.2	0.91	0.1 M KOH	Ref <sup>14</sup>

## References

1. S.-N. Zhao, J.-K. Li, R. Wang, J. Cai and S.-Q. Zang, Electronically and Geometrically Modified Single-Atom Fe Sites by Adjacent Fe Nanoparticles for Enhanced Oxygen Reduction, *Adv. Mater.*, 2022, **34**, 2107291.

2. K. Yuan, D. Lützenkirchen-Hecht, L. Li, L. Shuai, Y. Li, R. Cao, M. Qiu, X. Zhuang, M. K. H. Leung, Y. Chen and U. Scherf, Boosting Oxygen Reduction of Single Iron Active Sites via Geometric and Electronic Engineering: Nitrogen and Phosphorus Dual Coordination, *J. Am. Chem. Soc.*, 2020, **142**, 2404-2412.
3. J.-C. Li, H. Zhong, M. Xu, T. Li, L. Wang, Q. Shi, S. Feng, Z. Lyu, D. Liu, D. Du, S. P. Beckman, X. Pan, Y. Lin and M. Shao, Boosting the activity of Fe–Nx moieties in Fe–N–C electrocatalysts via phosphorus doping for oxygen reduction reaction, *Sci. China Mater.*, 2019, **63**, 965-971.
4. M. Wang, W. Yang, X. Li, Y. Xu, L. Zheng, C. Su and B. Liu, Atomically Dispersed Fe–Heteroatom (N, S) Bridge Sites Anchored on Carbon Nanosheets for Promoting Oxygen Reduction Reaction, *ACS Energy Lett.*, 2021, **6**, 379-386.
5. H. Adabi, A. Shakouri, N. Ul Hassan, J. R. Varcoe, B. Zulevi, A. Serov, J. R. Regalbuto and W. E. Mustain, High-performing commercial Fe–N–C cathode electrocatalyst for anion-exchange membrane fuel cells, *Nat. Energy*, 2021, **6**, 834-843.
6. J.-W. Huang, Y.-B. Chen, X.-L. Chen, X. Liu, L.-S. Ma, W.-Y. Su, Y. Zhao, H.-B. Zhu and H. Yang, Exploring Efficient Fe/N/C Electrocatalysts for Oxygen Reduction from Nonporous Interpenetrated Metal–Organic Framework Involving in Situ Formation of ZnO Templates, *ACS Sustainable Chem. Eng.*, 2020, **8**, 3208-3217.
7. Y. Zhang, Y. Zhao, M. Ji, H.-m. Zhang, M. Zhang, H. Zhao, M. Cheng, J. Yu, H. Liu, C. Zhu and J. Xu, Synthesis of Fe<sub>3</sub>C@porous carbon nanorods via carbonizing Fe complexes for oxygen reduction reaction and Zn–air battery, *Inorg. Chem. Front.*, 2020, **7**, 889-896.
8. X.-W. Song, S. Zhang, H. Zhong, Y. Gao, L. A. Estudillo-Wong, N. Alonso-Vante, X. Shu and Y. Feng, FeCo nanoalloys embedded in nitrogen-doped carbon nanosheets/bamboo-like carbon nanotubes for the oxygen reduction reaction, *Inorg. Chem. Front.*, 2021, **8**, 109-121.
9. J.-W. Huang, Y.-B. Chen, J.-M. Yang, H.-B. Zhu and H. Yang, Boosting the oxygen reduction performance of MOF-5-derived Fe-N-C electrocatalysts via a dual strategy of cation-exchange and guest-encapsulation, *Electrochim. Acta*, 2021, **366**, 137408.
10. Q. Wang, Y. Yang, F. Sun, G. Chen, J. Wang, L. Peng, W.-T. Chen, L. Shang, J. Zhao, D. Sun-Waterhouse, T. Zhang and G. I. N. Waterhouse, Molten NaCl-Assisted Synthesis of Porous Fe-N-C Electrocatalysts with a High Density of Catalytically Accessible FeN<sub>4</sub> Active Sites and Outstanding Oxygen Reduction Reaction Performance, *Adv. Energy Mater.*, 2021, **11**, 2100219.

11. T. Chen, J. Wu, C. Zhu, Z. Liu, W. Zhou, C. Zhu, C. Guan and G. Fang, Rational design of iron single atom anchored on nitrogen doped carbon as a high-performance electrocatalyst for all-solid-state flexible zinc-air batteries, *Chem. Eng. J.*, 2021, **405**, 125956.
12. G. Wang, J. Deng, T. Yan, J. Zhang, L. Shi and D. Zhang, Turning on electrocatalytic oxygen reduction by creating robust Fe–Nx species in hollow carbon frameworks via in situ growth of Fe doped ZIFs on g-C<sub>3</sub>N<sub>4</sub>, *Nanoscale*, 2020, **12**, 5601-5611.
13. X. Li, L. Ni, J. Zhou, L. Xu, C. Lu, G. Yang, W. Ding and W. Hou, Encapsulation of Fe nanoparticles into an N-doped carbon nanotube/nanosheet integrated hierarchical architecture as an efficient and ultrastable electrocatalyst for the oxygen reduction reaction, *Nanoscale*, 2020, **12**, 13987-13995.
14. Y. Huang, K. Liu, S. Kan, P. Liu, R. Hao, W. Liu, Y. Wu, H. Liu, M. Liu and K. Liu, Highly dispersed Fe-N<sub>x</sub> active sites on Graphitic-N dominated porous carbon for synergetic catalysis of oxygen reduction reaction, *Carbon*, 2021, **171**, 1-9.